HHS Public Access

Author manuscript

Angew Chem Int Ed Engl. Author manuscript; available in PMC 2019 June 06.

Published in final edited form as:

Angew Chem Int Ed Engl. 2017 August 21; 56(35): 10399–10402. doi:10.1002/anie.201704674.

Reconstitution of Low-Density Lipoproteins with Fatty Acids for the Targeted Delivery of Drugs into Cancer Cells

Chunlei Zhu,
The Wallace H. Coulter Department of Biomedical Engineering, Georgia Institute of Technology and Emory University, Atlanta, GA 30332 (USA)

Pallab Pradhan,
The Wallace H. Coulter Department of Biomedical Engineering, Georgia Institute of Technology and Emory University, Atlanta, GA 30332 (USA)

The Parker H. Petit Institute for Bioengineering and Biosciences, Center for ImmunoEngineering at Georgia Tech, Georgia Institute of Technology, Atlanta, GA 30332 (USA)

Da Huo,
The Wallace H. Coulter Department of Biomedical Engineering, Georgia Institute of Technology and Emory University, Atlanta, GA 30332 (USA)

Jiajia Xue,
The Wallace H. Coulter Department of Biomedical Engineering, Georgia Institute of Technology and Emory University, Atlanta, GA 30332 (USA)

Song Shen,
The Wallace H. Coulter Department of Biomedical Engineering, Georgia Institute of Technology and Emory University, Atlanta, GA 30332 (USA)

Krishnendu Roy, and
The Wallace H. Coulter Department of Biomedical Engineering, Georgia Institute of Technology and Emory University, Atlanta, GA 30332 (USA)

The Parker H. Petit Institute for Bioengineering and Biosciences, Center for ImmunoEngineering at Georgia Tech, Georgia Institute of Technology, Atlanta, GA 30332 (USA)

Younan Xia[*]
The Wallace H. Coulter Department of Biomedical Engineering, Georgia Institute of Technology and Emory University, Atlanta, GA 30332 (USA)

School of Chemistry and Biochemistry, School of Chemical and Biomolecular Engineering, Georgia Institute of Technology, Atlanta, GA 30332 (USA)

Abstract

Low-density lipoproteins (LDLs) represent a novel class of nanocarriers for the targeted delivery of therapeutics into aberrant cells that overexpress the LDL receptor. Here we report a facile procedure for reconstituting the hydrophobic core of LDLs with a binary fatty acid mixture.

[*] younan.xia@bme.gatech.edu.

Facilitated by the tumor targeting capability of the apolipoprotein, the reconstituted, drug-loaded LDLs can effectively target cancer cells that overexpress the LDL receptor while showing minor adverse impact on normal fibroblasts. According to a hypothesized mechanism, the reconstituted LDLs can also enable metabolism-triggered drug release while preventing the payloads from lysosomal degradation. This study demonstrates that LDLs reconstructed with fatty acids hold great promise to serve as effective and versatile nanocarriers for targeted cancer therapy.

Table of contents entry

Tumor-targeting nanocarriers: The hydrophobic core of native low-density lipoproteins (LDLs) can be reconstituted with naturally occurring fatty acids to facilitate a metabolism-triggered drug release for targeted cancer therapy.

Graphical Abstract

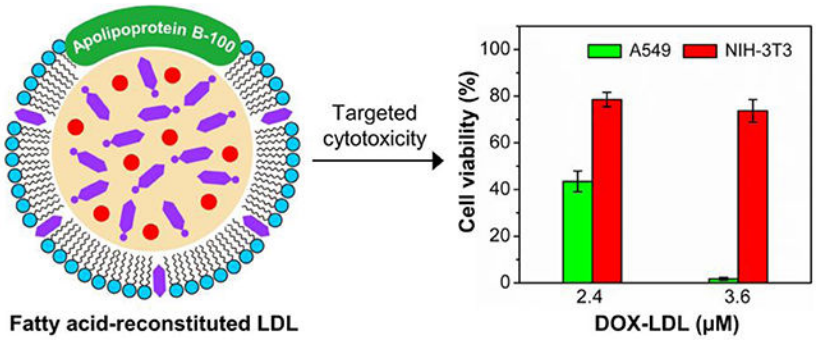

Keywords

low-density lipoproteins; fatty acids; eutectic mixture; drug delivery; cancer therapy

Low-density lipoproteins (LDLs) have been explored as a novel class of nanocarriers for targeted delivery of imaging contrast agents and therapeutics into aberrant cells owing to their small sizes (<50 nm), biodegradability, and long blood circulation time (2–4 days).[1] Structurally, each LDL has a unique, well-defined architecture constructed from an amphiphilic phospholipid monolayer and a hydrophobic core comprised of >45 wt.% cholesteryl ester.[1a,1c,2] Its surface is decorated by an apolipoprotein B-100 macromolecule that can be specifically recognized by the LDL receptor.[3] Upon binding between apolipoprotein B-100 and the receptor, endocytosis will be triggered to attain cholesterol intake. In contrast with normal tissues, the LDL receptor is up-regulated in many types of malignant cells or tissues.[4] This unique feature allows LDLs to serve as a class of natural nanocarriers for tumor-targeted drug delivery.

Currently, three strategies have been developed to introduce payloads into LDLs, including non-covalent intercalation into the phospholipid monolayer, encapsulation in the hydrophobic core, and covalent conjugation with the apolipoprotein.[1a,1b] Encapsulation in the core is particularly well-suited for drug delivery because of the simple procedure and relatively large loading capacity. The encapsulation process typically involves core

reconstitution that uses a nonpolar organic solvent to extract the hydrophobic lipids and subsequently refills the resultant void spaces with a mixture of cholesterol esters and drugs or cholesterol-drug conjugates. However, the presence of excess cholesterol in the bloodstream greatly increases the risk of forming atherosclerotic plaques in the aortic vasculature, which may cause fatal diseases such as myocardial infarction and stroke.[5] Therefore, the cholesterol/cholesteryl ester formulation should be avoided and preferably replaced with other naturally occurring compounds.

Fatty acids, an important source of stored energy in living organisms, have been exploited as a class of promising biomaterials owing to their biocompatibility and biodegradability.[6] In the present study, we used a mixture of fatty acids as the hydrophobic matrix to reconstitute the native LDLs through a core-loading approach (Figure 1 a). Differential scanning calorimetry (DSC) was used to measure the melting points of mixtures derived from lauric acid (m. p. = 45 °C) and stearic acid (m. p. = 69 °C). At a weight ratio of 4:1, we obtained a eutectic mixture with a sharp melting point at 39 °C (Figure 1 b), which is slightly higher than the normal temperature of human body (37 °C). As such, the payloads can be effectively encapsulated without prominent leakage until being triggered for release at the target site. It is worth noting that lauric acid has a favorable effect on the increase of “good” blood cholesterol (high-density lipoprotein), whereas stearic acid enables the decrease of “bad” blood cholesterol (LDL).[7] As such, these naturally occurring compounds can be considered as safe materials for the substitution of cholesterol ester in LDL reconstitution. We then adopted the Krieger’s method with minor modifications to reconstruct the core of native LDLs.[8] Specifically, the endogenous core lipids were extracted and then replaced with the eutectic mixture of lauric acid and stearic acid. Our quantitative analysis indicates that *ca.* 50 wt.% of the total cholesterols (including free cholesterol and cholesteryl ester) could be removed using this method, providing adequate spaces for subsequent core loading (Table S1). The structural stability of LDLs before and after reconstitution was also confirmed by UV/vis and circular dichroism (CD) spectra (Figure S1). The characteristic absorption peak of apolipoprotein B-100 at 280 nm and the unique spectrum of a primarily α-helical protein with a negative peak at *ca.* 210 nm were both preserved,[9] indicating that the reconstitution process did not alter the structure of apolipoprotein B-100. The payloads, together with the binary fatty acids, were then core-loaded into the LDLs. Under ambient conditions, the fatty acids became solidified, facilitating the entrapment of the payloads in the matrix. Since the hydrophobic cavity of native LDLs prefers to accommodate hydrophobic substances, the loading mechanism is supposed to be the hydrophobic interactions between fatty acids and the payloads.

The morphology and integrity of the resultant rLDLs were examined using transmission electron microscopy (TEM). Both C6-reconstituted LDLs (C6-LDLs) and DOX-reconstituted LDLs (DOX-LDLs) exhibited good dispersity and a spherical shape essentially identical to those of native LDLs, suggesting that the reconstitution process only had a negligible impact on the morphology of the initial template (Figure 1 c–e). We further quantified the size distribution of the resultant particles. Relative to native LDLs, the rLDLs were slightly enlarged in size (Figure S2). Meanwhile, a somewhat broader distribution in size was found for DOX-LDLs. The slight increase in particle size can be attributed to the overloading of fatty acids, as well as the difference in molecular stacking between fatty acids

and cholesteryl esters. The UV/vis spectra shown in Figure S3 confirm the presence of C6 and DOX, demonstrating that the payloads had been successfully loaded into the rLDLs. Further quantification indicates that the average numbers of C6, DOX, lauric acid, and stearic acid contained in each LDL particle were 10 ± 1, 25 ± 3, 1499 ± 138, and 264 ± 25, respectively (Table S2). Compared to C6, the loading capacity of DOX in the rLDLs was higher, which can be attributed to a stronger interaction between DOX and the fatty acids according to the principle of “like dissolves like”.

We next studied the difference in receptor-mediated uptake of C6-LDLs between cancerous and normal cells. An *in vitro* assay was performed using A549 lung cancer cells and NIH-3T3 fibroblast cells that overexpress and moderately express the LDL receptor, respectively.[10] After incubation for 3 h, we observed a substantial accumulation of C6-LDLs inside the A549 cells (Figure 2 a). The overlay image demonstrates that most C6-LDLs were co-localized with Lysotracker (late endosome/lysosome marker), suggesting that the particles entered cells *via* an endocytic pathway. The punctate green fluorescence in the periphery of the cells can be ascribed to the newly bounded C6-LDLs or early internalization events. In comparison, the fluorescence intensity of C6 in NIH-3T3 cells was much weaker than that in A549 cells (Figure 2 b). Moreover, the fluorescence signals could only be detected around the edge of the cell rather than the cytoplasm because of the relatively slow internalization and/or non-specific binding.

To verify that the internalization process was primarily mediated by the LDL receptor, we investigated the uptake of C6-LDLs in the presence of 20-fold excess of native LDLs (Figure 2 c and d). Receptor blocking greatly decreased the uptake of C6-LDLs in both A549 and NIH-3T3 cells, with barely noticeable fluorescence in the cytoplasm. To quantify the differential receptor-mediated uptake in both cell lines, flow cytometric analysis was performed. As shown in Figure 2 e and f, there was a more pronounced peak shift for A549 cells than NIH-3T3 cells after incubation with C6-LDLs, indicating the targeting selectivity of rLDLs toward cancer cells over normal cells. In the presence of 20-fold excess of native LDLs, the population of both A549 and NIH-3T3 cells substantially shifted toward the direction with low fluorescence intensities. Further quantification indicates that after receptor blocking, there was 60-fold and 3-fold decrease in mean fluorescence intensity for A549 and NIH-3T3 cells, respectively (Figure S4). The data confirms that the rLDLs maintain the biological functions of native LDLs and still have a preferential affinity toward cancer cells that overexpress the LDL receptor.

We then investigated the intracellular drug delivery using DOX-LDLs. As shown in Figure 3 a and b, the A549 cells exhibited punctate red fluorescence, whereas the fluorescence signal was barely detected from the NIH-3T3 cells. This finding further confirms the higher affinity of DOX-LDLs toward cancer cells. It is worth noting that the fluorescence signals of DOX in some A549 cells were overlaid with the nuclei rather than being clustered in the cytoplasm, indicating the translocation of DOX into the nuclei. After internalization, the DOX-LDLs would be transported to the endo/lysosomes. Since fatty acids cannot be hydrolyzed, the therapeutic drugs are supposed to be protected from lysosomal degradation. However, cancer cells have an elevated energy demand to maintain rapid proliferation.[11] This, in turn, triggers the release of the fatty acids and payloads. Over time, the released

DOX intercalates into the deoxyribonucleic acids (rich in the nuclei) to inhibit the proliferation of cancer cells.

We then measured the release profile of DOX from the DOX-LDLs in phosphate buffered saline. As shown in Figure S5, the DOX exhibited a limited and sustained release behavior over 24 h. We hypothesized that both the phospholipid shell and the fatty acid core could act as a physical barrier to slow down the drug release. To quantitatively evaluate the targeted toxicity of DOX-LDLs, we performed cell viability analyses. Figure 3 c shows the dose-dependent growth inhibition of the DOX-LDLs on A549 cells. As the concentration of DOX-LDLs increased, the cell viability decreased significantly. When the concentration of DOX in DOX-LDLs reached 3.6 μM, the inhibitory rate was as high as 98%. The IC50 value was determined to be 2.3 μM, which was much lower than that of free DOX (14.6 μM), indicating the efficacy of the proposed metabolism-triggered drug release (Figure S6). In contrast, NIH-3T3 cells exhibited a resistance to DOX-LDLs under all tested concentrations as a result of the limited uptake of the rLDLs. Even for the group with the highest amount of DOX, NIH-3T3 cells still showed a survival rate of >70%.

We have also sought to simplify the delivery system by using just one of the fatty acids. However, the LDLs reconstituted from either lauric acid or stearic acid could not efficiently trap the DOX molecules due to the high crystallinity associated with single-component fatty acid, which results in drug efflux during solvent evaporation (Table S3). The binary fatty acid mixture could reduce the crystallinity of the system and thus keep drugs in the solid matrix. In addition, even under the same DOX concentrations, both lauric acid and stearic acid exhibited less prominent cytotoxicity against A549 cells, which is probably due to the ineffective drug release from a solid matrix with an elevated melting point (Figure S7). Taken together, it is necessary to manipulate the thermal properties of fatty acids to facilitate rapid and efficient drug release.

To verify the LDL receptor-mediated cytotoxicity, we conducted a receptor blocking assay with 20-fold excess of native LDLs. As shown in Figure 3 d, the competitive binding remarkably suppressed the cytotoxicity of DOX-LDLs toward A549 cells, and the cell viability was recovered to the same level as that of excess LDLs alone. However, we did not observe any increased survival rate for the blocking group of NIH-3T3 cells. Conversely, the excess LDLs and cytotoxic DOX-LDLs imposed a concerted inhibitory effect on the viability of NIH-3T3 cells. The cell survival condition was also examined using inverted optical microscopy (Figure S8). For the group incubated with DOX-LDLs, A549 cells exhibited an apoptotic phenotype with a highly shrunk and rounded shape. Receptor blocking with excess LDLs greatly rescued the cells to a healthy living status. As for NIH-3T3 cells, no obvious cell apoptosis was found for all groups, suggesting that the internalized DOX molecules were not enough to initiate noticeable cytotoxicity.

We also evaluated *in vivo* accumulation of the fatty acid-reconstituted LDLs in B16-F10 melanoma-bearing mice as the LDL receptor is known to be upregulated in melanoma cells. [12] We first confirmed the receptor-mediated uptake of the rLDLs using B16-F10 murine melanoma cells *in vitro* (Figure S9). To facilitate *in vivo* fluorescent detection, a near-infrared dye, IR780 iodide (IR780), was incorporated into LDLs to obtain IR780-LDLs,

which were then used for the study of *in vivo* biodistribution and competitive binding in subcutaneous B16-F10 melanoma-bearing C57BL/6 mice. As shown in Figure 4 a, the IR780-LDLs were able to accumulate in the solid tumors, and co-injection of IR780-LDLs and 20-fold excess of native LDLs significantly reduced their enrichment at these sites. We further quantified the average radiant efficiency (ARI) in these tumors. As shown in Figure 4 b, receptor blocking by excess LDLs resulted in a 2.2-fold decrease in ARI, indicating that the receptor-mediated endocytosis probably plays a primary role in the uptake of these nanoparticles. The distribution of IR780-LDLs in major organs was also examined (Figure S10). Since the B16-F10 melanoma has a black color, both the excitation light and fluorescence signals of IR780 were greatly attenuated due to its self-absorption. As such, it is difficult to make parallel comparison between the major organs and the tumor based on the ARI. Nevertheless, the data shown in Figure 4 suggest that the biological functions of rLDL was maintained and the rLDLs can be used to target tumors that overexpress the LDL receptor.

In summary, LDLs reconstituted from a binary fatty acid mixture have been developed as a biocompatible, tumor-targeting nanocarrier for the delivery of both imaging contrast agents and anti-cancer drugs. The reconstitution process has essentially no impact on the morphology and biological functions of LDLs. In terms of using fatty acid as a matrix for drug loading, there are a number of advantages. Firstly, fatty acids are naturally occurring biomolecules, indicating good biocompatibility and biodegradability. Secondly, fatty acids are an important class of fuel source. Since the rapidly proliferating cancer cells have a higher demand on energy, we hypothesize that the metabolism-triggered drug release will be augmented. Thirdly, all molecules transported to lysosomes are inevitably hydrolyzed into reusable small units. Fatty acids, the smallest units in lysosomes, are supposed to protect the payloads from hydrolysis and thus facilitate endo-lysosomal escape. All these features contribute to the rapid and effective cytotoxicity toward cancer cells, making the fatty acid-reconstituted LDLs a promising nanocarrier for targeted cancer therapy.

Supplementary Material

Refer to Web version on PubMed Central for supplementary material.

Acknowledgements

This work was supported in part by a grant from the National Institutes of Health (R01 CA138527) and startup funds from the Georgia Institute of Technology (to Y.X. and K.R.).

References

[1]. a) Ng KK, Lovell JF, Zheng G, Acc. Chem. Res 2011, 44, 1105–1113; [PubMed: 21557543] b) Harisa GI, Alanazi FK, Saudi. Pharm. J 2014, 22, 504–515; [PubMed: 25561862] c) Huang H, Cruz W, Chen J, Zheng G, Wiley Interdiscip. Rev.: Nanomed. Nanobiotechnol. 2015, 7, 298–314.

[2]. Gotto AM, Pownall HJ, Havel RJ, Methods Enzymol. 1986, 128, 3–41. [PubMed: 3523141]

[3]. a) Veniant MM, Nielsen LB, Boren J, Young SG Trends Cardiovasc. Med 1999, 9, 103–107; [PubMed: 10578525] b) Segrest JP, Jones MK, De Loof H, Dashti N, J. Lipid Res 2001, 42, 1346–1367. [PubMed: 11518754]

[4]. a) Vitols S, Cancer Cells 1991, 3, 488–495; [PubMed: 1840290] b) Firestone RA, Bioconjug. Chem 1994, 5, 105–113. [PubMed: 8031872]

[5]. a) Berliner J, Heinecke J, Free Radical Biol. Med 1996, 20, 707–727; [PubMed: 8721615] b) Libby P, Aikawa M, Schönbeck U, Biochim. Biophys. Acta 2000, 1529, 299– 309; [PubMed: 11111097] c) Packard R, Libby P, Clin. Chem 2008, 54, 24–38. [PubMed: 18160725]

[6]. a) Xie S, Zhu L, Dong Z, Wang X, Wang Y, Li X, Zhou W, Colloids Surf. B Biointerfaces 2011, 83, 382–387; [PubMed: 21215599] b) Chirio D, Gallarate M, Peira E, Battaglia L, Serpe L, Trotta M, J. Microencapsul 2011, 28, 537–548; [PubMed: 21702702] c) Kumara S, Randhawa JK, RSC Adv. 2015, 5, 68743–68750.

[7]. a) Mensink RP, Zock PL, Kester ADM, Katan MB, Am. J. Clin. Nutr 2003, 77, 1146–1155; [PubMed: 12716665] b) Hunter JE, Zhang J, Kris-Etherton PM, Am. J. Clin. Nutr 2010, 91, 46–63. [PubMed: 19939984]

[8]. Krieger M, Methods Enzymol. 1986, 128, 608–613. [PubMed: 3724525]

[9]. a) Paananen K, Saarinen J, Annila A, Kovanen PT, J. Biol. Chem 1995, 270, 12257–12262; [PubMed: 7744877] b) Ahmad S, Akhter F, Moinuddin, Shahab U, Khan MS, Int. J. Biol. Macromol 2013, 62, 167–171. [PubMed: 24012841]

[10]. Gueddari N, Favre G, Hachem H, Marek E, Le Gaillard F, Soula G, Biochimie 1993, 75, 811–819. [PubMed: 8274533]

[11]. Pfeiffer T, Schuster S, Bonhoeffer S, Science 2001, 292, 504–507. [PubMed: 11283355]

[12]. a) Ponty E, Favre G, Benaniba R, Boneu A, Lucot H, Carton M, Soula G, Int. J. Cancer 1993, 54, 411–417; [PubMed: 8509217] b) Versluis AJ, van Geel PJ, Oppelaar H, van Berkel TJ, Bijsterbosch MK, Br. J. Cancer 1996, 74, 525–532. [PubMed: 8761365]

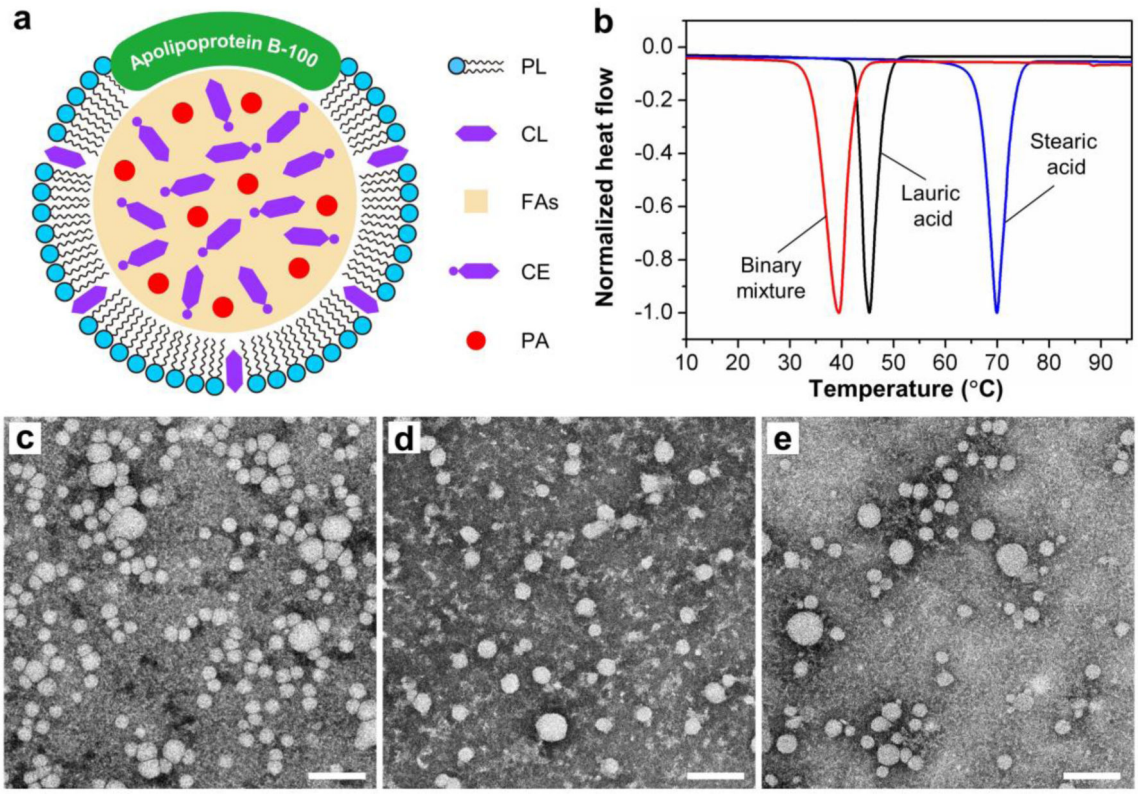

Figure 1.

a) Schematic illustration showing a low-density lipoprotein (LDL) nanoparticle whose core has been reconstituted with a drug-loaded mixture of fatty acids. Abbreviations: PL, phospholipid; CL, cholesterol; FAs, fatty acids; CE, cholesteryl ester; PA, payload. b) DSC curves of lauric acid, stearic acid, and a binary mixture of lauric acid and stearic acid at a weight ratio of 4:1. c–e) TEM images of (c) native LDLs, (d) C6-LDLs, and (e) DOX-LDLs. These nanoparticles were negatively stained with 2 wt.% aqueous phosphotungstic acid prior to characterization. Scale bars: 100 nm.

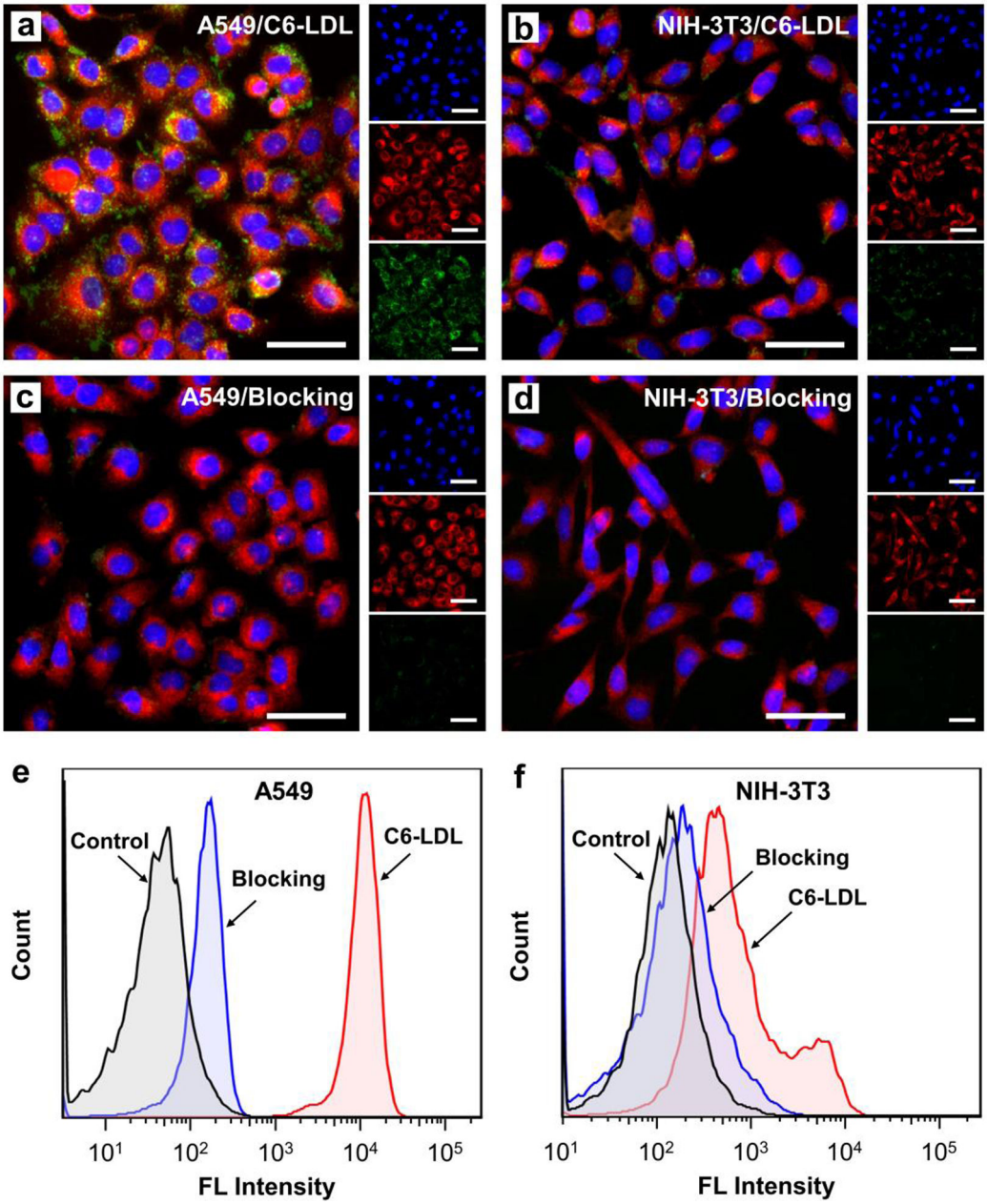

Figure 2.

A comparison of the uptakes of C6-LDLs by A549 and NIH-3T3 cells. a, b) Uptake of C6-LDLs by (a) A549 and (b) NIH-3T3 cells. c, d) Receptor blocking in (c) A549 and (d) NIH-3T3 cells using 20-fold excess of native LDLs. The nuclei were stained with Hoechst 33342 and are shown in blue; the lysosomes were stained with Lysotracker and are shown in red; and C6 is shown in green. Scale bars: 50 μm. e, f) Flow cytometric analysis of LDL receptor-mediated uptake in (e) A549 and (f) NIH-3T3 cells.

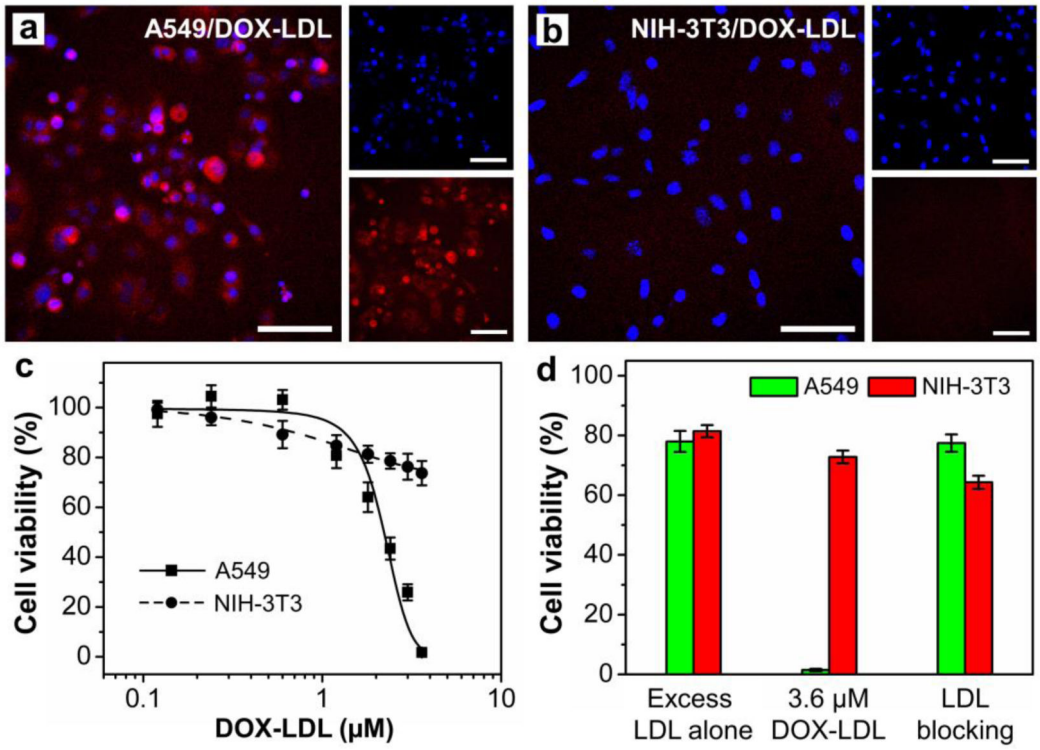

Figure 3.

LDL receptor-mediated, targeted delivery of DOX-LDLs into A549 cells in comparison with NIH-3T3 cells. a, b) A comparison of the delivery of DOX-LDLs into (a) A549 and (b) NIH-3T3 cells. The nuclei were stained with Hoechst 33342 and are shown in blue; DOX is shown in red. Scale bars: 50 μm. c) Cytotoxicity of DOX-LDLs towards A549 and NIH-3T3 cells. d) Cytotoxicity of DOX-LDLs toward A549 and NIH-3T3 cells in the absence or presence of native LDLs in 20-fold excess. “Excess LDL alone” indicates 20-fold excess of native LDLs alone, whereas “LDL blocking” represents a mixture of 20-fold excess of native LDLs and 3.6 μM DOX-LDLs.

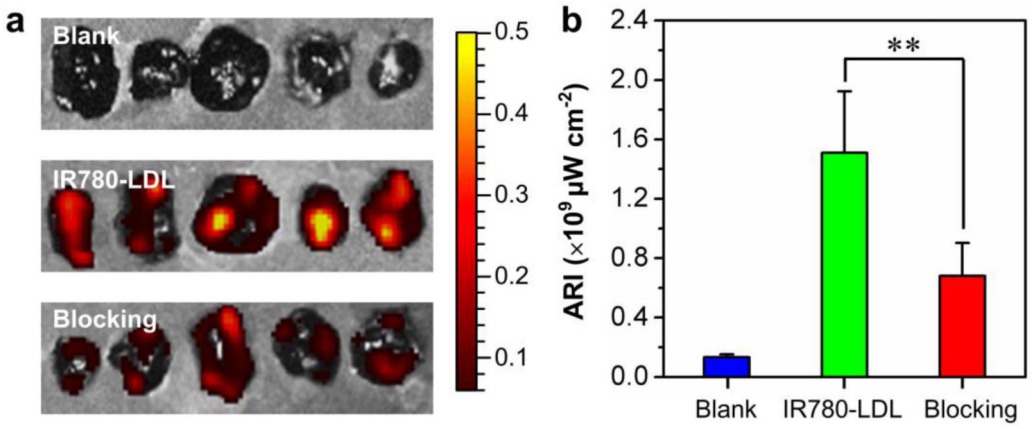

Figure 4.

In vivo evaluation of IR780-LDL accumulation in B16-F10 melanoma. a) Fluorescence images of the tumors excised at 24 h post intravenous injection and b) the corresponding average radiant efficiency (ARI). “Blank”, “IR780-LDL”, and “Blocking” indicate the LDLs reconstituted with binary fatty acids alone, the rLDLs loaded with both binary fatty acids and IR780, and a mixture of IR780-LDLs and 20-fold excess of native LDLs, respectively. The color bar in (a) represents the radiant efficiency ($\times 10^9$ μW cm^{-2}). Significant difference between the tumors with or without receptor blocking is indicated (**, $p < 0.005$).